Role of the countercations on the molecular sieve properties of a clinoptilolite

Article *in* Microporous Materials · August 1996

DOI: 10.1016/0927-6513(96)00022-3

ELSEVIER

Microporous Materials 7 (1996) 1–13

MICROPOROUS
MATERIALS

Role of the countercations on the molecular sieve properties of a clinoptilolite

A. Arcoya [a], J.A. González [b], G. Llabre [b], X.L. Seoane [a,*], N. Travieso [b]

[a] *Instituto de Catálisis y Petroleoquímica, CSIC, Campus Universidad Autónoma, Cantoblanco, 28049-Madrid, Spain*
[b] *Centro de Investigaciones Químicas, Washington 169, Cerro, La Habana, Cuba*

Received 4 July 1995; accepted 12 January 1996

Abstract

Samples of clinoptilolite enriched with Na^+, K^+, Cs^+, NH_4^+, Ca^{2+}, Mg^{2+}, and Ba^{2+} cations were prepared by ion-exchange. The degree of exchange for the different samples is discussed in terms of location and diffusivity of the cations. The thermal stability of natural clinoptilolite and of the enriched forms, as determined by XRD, is related to the nature and location of the major countercation in the zeolite framework. The specific retention volumes of O_2, N_2, CO and CH_4 on each sample and the adsorption enthalpies of these gases were measured by a chromatographic method in the range of 298–393 K. The results are explained on the basis of the strength of the interaction molecule-adsorption sites of the zeolite, taking into account the diffusivity of gas molecules through the zeolite channels, and their accessibility to the adsorption sites, according to the more probable location of the cation in the lattice.

Keywords: Clinoptilolite; Ion-exchange; Enthalpies of gas adsorption; Gas adsorption; Molecular sieves; Properties

1. Introduction

The use of natural zeolites as gas adsorbents has a great commercial interest due to their availability and low cost. Molecular sieve properties of clinoptilolite (CLI), which is the most abundant zeolite in nature, have been investigated for molecules of different dimensions [1–4]. Since the nature of the countercations can significantly affect these properties [1,3], ion exchange with protons and different cations has been frequently used as a method to enhance the adsorptive capacity of clinoptilolite toward different molecules, including O_2 and N_2 [5–7].

The separation efficiency of zeolites in chromatographic processes is governed by both the strength of the sorbate–adsorbent interactions and the molecular diffusion rate through the pores [8]. However, few studies have been made on this topic for clinoptilolite type zeolites. Barrer and Coughlan [2] have studied the adsorption of a non-polar molecule (Kr), a molecule with a quadrupole moment (CO_2), and one with a dipole moment (H_2O). Diffusion and adsorption of N_2 and CH_4 on K-, Na-, H-, Ca- and Mg-CLI have been analyzed by Ackley and Yang [9,10], who correlate selectivity for N_2/CH_4 kinetic separation with type, size and location of cations in the channels of the zeolite. Furthermore, Ackley et al. [11] found that the effect of the location of the major countercation upon diffusion and separation

* Corresponding author.

PII S0927-6513(96)00022-3

of these gases is higher than that of its size and concentration.

In a previous paper [12] we have studied the physicochemical and catalytic properties of a protonated clinoptilolite from the deposit of Castilla (Cuba). The present work deals with the capability of the natural clinoptilolite exchanged with ammonium, alkaline and alkaline-earth cations, for the separation of methane, oxygen, nitrogen, and carbon monoxide. These gases have different polarizabilities, electric multipole moments and molecular sizes, the last being, however, comparable to the effective dimension of the channels reported for the different cationic forms of clinoptilolite [11]. In addition, the adsorption and/or selective separation of these gases is a process of significant technological interest [7,11]

The gas-chromatographic retention volumes and the adsorption enthalpies of CO, O_2, N_2 and CH_4 on the different samples were experimentally determined and are discussed in terms of polarizability of the gases, polarizing power of the cations and their location in the zeolite framework. The potential of the raw material and prepared samples as adsorbents in gas separation and/or purification of air is examined.

2. Experimental

2.1. Preparation of the samples

Natural clinoptilolite from Castilla (Cuba) has a purity of more than 85%, mordenite, calcite and quartz being the major impurities [12]. Its chemical composition (wt.-%) is: SiO_2 68.05; Al_2O_3 12.3; TiO_2 0.40; Fe_2O_3 1.34; CaO 3.70; MgO 1.03; Na_2O 0.43; K_2O 1.70 and H_2O 11.06. The material (particle size 0.2–0.5 mm), was contacted with 0.1 M sodium acetate solution, to remove carbonate species, and then washed with distilled water and dried at 393 K overnight.

The cationic samples were prepared from CLI by ion exchange with 2 N aqueous solutions of NH_4^+, Na^+, K^+, Cs^+, Mg^{2+}, Ca^{2+}, and Ba^{2+} chlorides, respectively (10 ml solution/g mineral) at reflux temperature for 84 h. During the exchange, aliquot portions were periodically taken from the treatment solution to determine by atomic absorption spectrophotometry the extracted amount of Na^+, K^+, Mg^{2+}, and Ca^{2+} cations. The solids were filtered, washed with distilled water until the Cl^- ions were totally removed, dried at 393 K and stored in a desiccator. The chemical composition of the samples in oxide wt.-% (dry basis) is given in Table 1.

2.2. Gas-chromatographic measurements

Gas-chromatographic measurements were carried out in a PYE 304 gas chromatograph fitted with a thermal conductivity detector and an electronic integrator, using H_2 as carrier gas (50 $cm^3 \cdot min^{-1}$). The TC detector temperature was 413 K and the filaments current 260 Ma. Samples of 12 g of zeolite were introduced into stainless steel columns of 1 m length and 6.35 mm OD and activated under a flow of 20 $ml \cdot min^{-1}$ of N_2 prior to the chromatographic measurement.

The effect of the activation conditions of the sample CLI (553–723 K and 0.5–11 h) on the separation N_2/O_2, was investigated using air as a model mixture. For the chromatographic measurements, O_2, N_2, CH_4, CO or air (GC grade) were introduced into the column by a gas valve loop of 0.5 ml. The retention times were measured at column temperatures in the range of 298–393 K. H_2 and N_2 were successively passed through an Oxytrap purifier and a 5A molecular sieve filter.

2.3. Thermogravimetric measurements

In order to examine the influence of the water content on the resolution power of the natural clinoptilolite activated at different temperatures, the final water content of each sample was determined by thermogravimetric analysis, in a Mettler TA-3000 system. Portions of 100 mg of CLI were heated at 10 $K \cdot min^{-1}$ in a dry N_2 stream up to the relevant activation temperature and maintained at this temperature during 8 h. The weight loss was continually recorded, and the final hydration degree related to that of the natural material was calculated.

Table 1
Chemical composition (wt.-%) of the enriched clinoptilolites (dry samples)

Sample	NH_4^+	Na_2O	K_2O	Cs_2O	MgO	CaO	BaO	SiO_2	Al_2O_3
CLI	0.00	0.48	1.91	0.00	1.16	4.16	0.00	76.51	13.80
NH_4-CLI	2.19	0.00	0.60	0.00	0.26	0.41	0.00	79.94	14.38
Na-CLI	0.00	4.45	1.68	0.00	0.93	1.22	0.00	75.75	13.86
K-CLI	0.00	0.08	10.03	0.00	0.24	0.92	0.00	73.34	13.35
Cs-CLI	0.00	0.00	0.29	5.62	0.17	0.58	0.00	60.61	11.03
Mg-CLI	0.00	0.13	1.52	0.00	2.53	3.01	0.00	76.82	13.84
Ca-CLI	0.00	0.01	1.56	0.00	0.70	5.53	0.00	76.26	13.76
Ba-CLI	0.00	0.00	0.78	0.00	0.25	0.77	14.52	69.23	12.52

2.4. XRD measurements

In order to detect possible structural changes produced by thermal activation, X-ray diffraction patterns of the natural and cation-exchanged clinoptilolites activated at different temperatures were obtained with a Philips PW-1710 powder diffractometer, using CuKα radiation at 40 kV and 20 mA, and nickel filter.

3. Structure of clinoptilolite

According to the literature [13–15] the structure of clinoptilolite consists of a two-dimensional system of three types of channels: two parallel channels, A (10-member ring) and B (8-member ring), perpendicularly intersected by channels C (8-member ring), with sizes of 4.4×7.2 Å, 4.1×4.7 Å and 4.0×5.5 Å, respectively. A view of the clinoptilolite structure, including the cation sites, based on the structure given by Koyama and Takeuchi [14], is shown in Fig. 1. The main cation positions in this structure are:

M(1), located in channel A, coordinated with two framework oxygen atoms and five H_2O molecules. One of these molecules may not be directly associated to M(1), giving a pseudo-octahedral system [14]. This site is occupied by Ca^{2+} and preferably by Na^+.

M(2), situated in channel B, is coordinated by three framework oxygen atoms and five H_2O molecules. M(2) is occupied by Na^+ and preferably C a^{2+}.

M(3), in channel C, is coordinated by six framework oxygen atoms and three H_2O molecules, and it is occupied by K^+ and, probably, Ba^{2+} [16,17]. Because this position is very close to M(1), a simultaneous occupancy of both sites is not possible.

M(4), which is located in channel A like M(1), but at a center of inversion. Its octahedral coordination is achieved by six H_2O molecules. The occupancy of this position is low, and corresponds to Mg^{2+}.

4. Results and discussion

4.1. Ion exchange

The plots in Fig. 2 show the exchange degree of each cation clinoptilolite by NH_4^+ as a function of the time of treatment. The degree of exchange for a cation i is defined as $X_i = 100C_{i,t}/C_{i,0}$, $C_{i,t}$ being the number of equivalents of i extracted at time t and $C_{i,0}$ the number of equivalents of i present in the untreated sample. After 72 h (t_∞), the rate of exchange is practically negligible, indicating that an equilibrium of exchange has been reached. For sodium and calcium present in the natural zeolites (Na_Z^+ and Ca_Z^{2+}, respectively), the degree of exchange at equilibrium (X_e) is higher than 90% of its theoretical exchange capacity, whereas for Mg_Z^{2+} and K_Z^+ the equilibrium is attained after 70% of these cations is removed.

Similar types of curves were obtained for the exchange with the other cations, although both the value of X_e for each countercation (Table 2) and the total content of the loaded cation (Table 3:

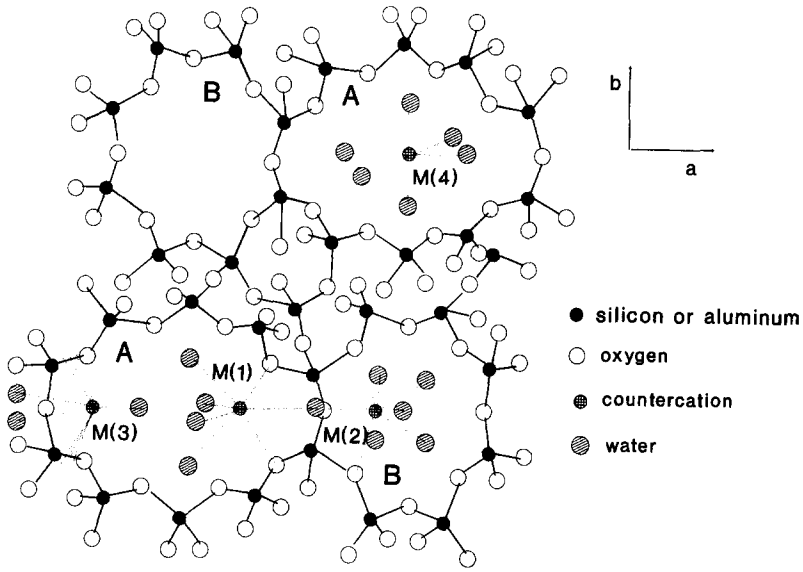

Fig. 1. The *c*-axis projection of the structure of clinoptilolite, showing the cation.

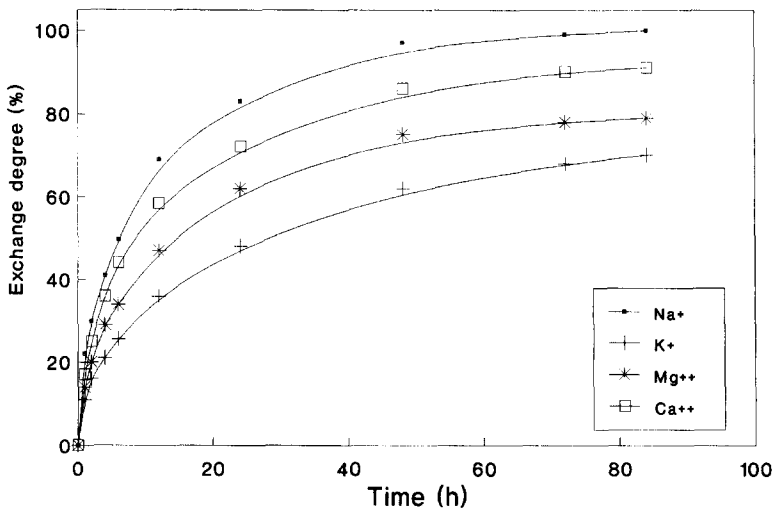

Fig. 2. Degree of exchange of the clinoptilolite countercations by ammonium as a function of the time of treatment.

TCLC = number of equivalents of the loaded cation × 100/MEC, where MEC = maximum ion-exchange capacity of the CLI per unit cell = 6.22 equiv./uc, based on O = 72) depend on the nature of the in-going cation. These differences are probably related to the location of the cations in the lattice of the clinoptilolite. Note, for example, that Mg-CLI is the less enriched form probably because Mg^{2+} is located in M(4), which is a low occupancy site. Na^+ and Ca^{2+}, located in M(1) and M(2) positions, are the more easily extracted cations (Table 2) but they are also the more difficult to incorporate, as shown by the values of M^{n+} (Table 3). M^{n+} is the amount of a given cation (in equiv./uc) incorporated into the zeolite by ion exchange. If M^{n+} is Na, K, Mg or Ca, the total content of this cation in each enriched sample will be: M^{n+} (column 2) + $C_{i,0}$ (line 1: CLI). On

Table 2
Initial rate of extraction and degree of ion-exchange at equilibrium of the cations [a]

Sample	Ca_Z^{2+}		Na_Z^{+}		Mg_Z^{2+}		K_Z^{+}	
	r_0	X_e (%)	r_0	X_e (%)	r_0	X_e (%)	r_0	X_e (%)
NH_4-CLI	0.173	91	0.014	100	0.048	79	0.009	70
Na-CLI	0.156	72	–	–	0.007	19	0.003	12
K-CLI	0.513	78	0.035	83	0.104	78	–	–
Cs-CLI	0.453	83	0.030	100	0.026	82	0.017	81
Mg-CLI	0.068	31	0.010	72	–	–	0.004	20
Ca-CLI	–	–	0.006	97	0.010	33	0.002	18
Ba-CLI	0.156	80	0.019	100	0.030	76	0.008	56

[a] r_0: initial rate of exchange (mequiv. g_Z^{-1} h^{-1}). X_e: degree of exchange (%) at equilibrium.

Table 3
Cation content per unit cell in the enriched clinoptilolites

Sample	M^{n+} [a]	Countercation content (equiv./uc)							
		NH_4^+	Na^+	K^+	Cs^+	Mg^{2+}	Ca^{2+}	Ba^{2+}	TCLC [b]
CLI	0	0.00	0.36	0.96	0.00	1.32	3.60	0.00	–
NH_4-CLI	5.35	5.35	0.00	0.28	0.00	0.28	0.32	0.00	86.0
Na-CLI	2.97	0.00	3.30	0.82	0.00	1.06	1.00	0.00	53.0
K-CLI	4.13	0.00	0.06	5.07	0.00	0.28	0.78	0.00	82.0
Cs-CLI	5.24	0.00	0.00	0.18	5.24	0.24	0.60	0.00	85.0
Mg-CLI	1.55	0.00	0.10	0.74	0.00	2.88	2.46	0.00	46.5
Ca-CLI	0.96	0.00	0.01	0.76	0.00	0.88	4.54	0.00	75.3
Ba-CLI	4.80	0.00	0.00	0.42	0.00	0.32	0.70	1.80	77.0

[a] equiv. of each cation incorporated per uc.
[b] TCLC = total content of loaded cation (equiv. of the loaded cation × 100/MEC, where MEC = maximum ion-exchange capacity of the CLI per unit cell: 6.22 equiv./uc, based on O = 72).

the other hand, zeolites in which the major cation seems to go to M(3) are the more enriched forms (K-, Cs- and Ba-CLI). The fact that a highly enriched Cs-CLI is obtained by ion exchange (see Table 2), suggests that Cs^+ probably also goes to the M(3) position. This location is consistent with the rule suggested by Sugiyama and Takeuchi [17]: "upon replacement of cations in natural heulandites, the large monovalent cations are first concentrated at M(3)", even if Smyth et al. [18] located Cs^+ at five different positions.

From the slope of the exchange curves at $t \rightarrow 0$, the initial exchange rate (r_0) for each countercation was calculated (Table 2) by the equation

$$r_0 = dC_i/dt = (C_{i,0}/100)dX_i/dt \text{ at } t \rightarrow 0 \quad (1)$$

In all cases, the initial exchange rate of the exit cation follows the sequence $Ca_Z^{2+} > Mg_Z^{2+} > Na_Z^{+} > K_Z^{+}$. With regard to the in-going cation, the initial rate of extraction of Ca_Z^{2+} and Na_Z^{+} the sequence is $Cs^+ = K^+ > NH_4^+ > Na^+ = Ba^{2+} > Mg^{2+} > Ca^{2+}$. In addition to the location of the countercation in the lattice, the exchange rate depends also on the geometry of the clinoptilolite channels and the diffusivity of the incorporated cation. So, the plots of ion exchange degree $NH_4^+ \leftrightarrow M_Z^{n+}$ for each cation against $t^{1/2}$, at least for the small values of t, fit the kinetic equation

$$C_{i,t}/C_{i,0} = A_i(D_i/\pi)^{1/2}(t^{1/2}) \quad (2)$$

(see Fig. 3), as expected for processes controlled by intracrystalline diffusion [1]. In Eq. 2, A_i is a constant and D_i the intracrystalline diffusion coefficient or diffusivity. Due to the complexity of

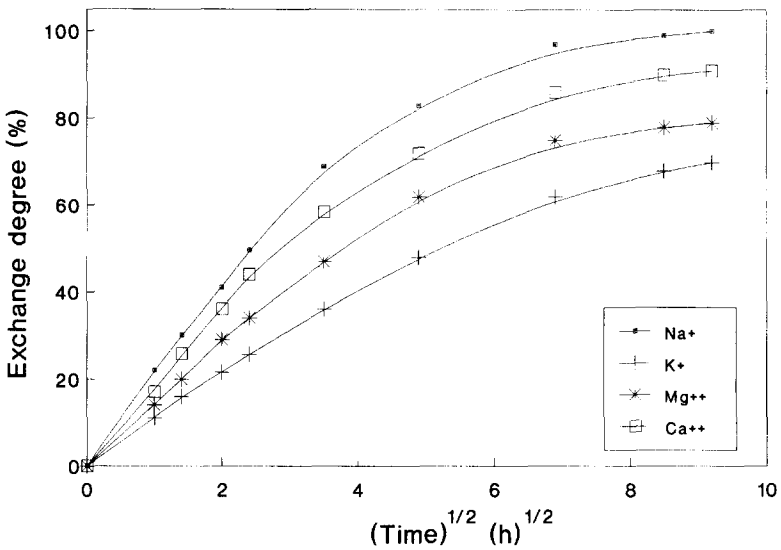

Fig. 3. Kinetics of the exchange $M_Z^{n+} \rightleftharpoons NH_4^+$ in clinoptilolite.

the ion exchange process, Eq. 2 is only an approximate relationship and deviations from the straight line are observed at longer times. From the slope of the linear portion of the curves, the diffusivity of the exit cations can be calculated. The cation diffusion is governed by the strength of the interaction of the exit cation with structure oxygens, which increases with the *polarizing power of the cations* (ϕ), *i.e., the charge to ionic radius ratio* (Table 4). Consequently, the higher the polarizing power the lower the diffusivity, such as it occurs for Na^+, Ca^{2+} and Mg^{2+}. The anomalous behaviour exhibited by K_Z^+, for which the diffusivity should be higher, indicates that the exit rate of K_Z^+ depends also on other factors, such as its position in the channels of the zeolite.

Table 4
Physical characteristics of the cations

Cation	Ionic radius (Å)	ϕ [a]
H^+	–	–
Na^+	0.95	1.05
K^+	1.33	0.75
Cs^+	1.69	0.59
Mg^{2+}	0.65	3.08
Ca^{2+}	0.99	2.02
Ba^{2+}	1.35	1.48

[a] ϕ = polarizing power of the cations = ionic charge/ionic radius.

From the data in Table 2, one can deduce that extraction of K_Z^+ is more limited on Ca-, Na- and Mg-CLI than on the other samples. This result is probably due to the fact that the location of Ca_Z^{2+} and Na_Z^+ in M(1) and M(2), and Mg_Z^{2+} in M(4), brings about a decrease of the effective free dimensions of the channels, as will be shown later.

4.2. Thermal activation of the samples

It is known that the presence of highly hydrated countercations (Ca_Z^{2+} and Mg_Z^{2+}) in clinoptilolite blocks the channels and, consequently, hinders the free traffic of the guest molecules [19]. Tsitsishvili et al. [19,20] have reported that thermal activation of the raw material below 573 K does not completely remove the water molecules arranged near these cations. For this reason, and in order to define the best conditions of activation, several portions of CLI were heated at different temperatures in the range of 553–873 K, for different periods of time. The water content of these samples was determined and their molecular sieve capacity evaluated in the O_2/N_2 separation from air. The efficiency for this process is defined by the 'resolution power' ($R_{O/N}$), which is calculated by the expression

$$R_{O/N} = 2d_{O-N}/(\delta_O + \delta_N) \quad (3)$$

where d_{O-N} is the distance between the maxima of the chromatographic peaks of O_2 and N_2, and δ_O and δ_N the half-width of such peaks, respectively. An efficient separation is reached for $R_{O/N} \geq 1.5$ [21]. The plots in Fig. 4 show both the resolution power and the dehydration degree of CLI as a function of the activation temperature. The highest values of $R_{O/N}$ (ca. 2) are achieved with the samples heated in the range 673–773 K. Activation temperatures above 773 K do not improve the separation efficiency. A certain parallelism is observed between the resolution power and the dehydration degree of the samples (Figs. 4 and 5). Actually, only after about 75% of the water is eliminated, do the samples show any resolution power, the more efficient ones are those dehydrated above 90%. This dehydration level is reached when the sample is heated within the optimal range of treatment temperatures. Note that the dehydration curve as a function of temperature does not show any discontinuity, as was also observed by Ward and McKague [22] for Hector clinoptilolite. Such parallelism probably is a consequence of the greater space availability in the inner channels

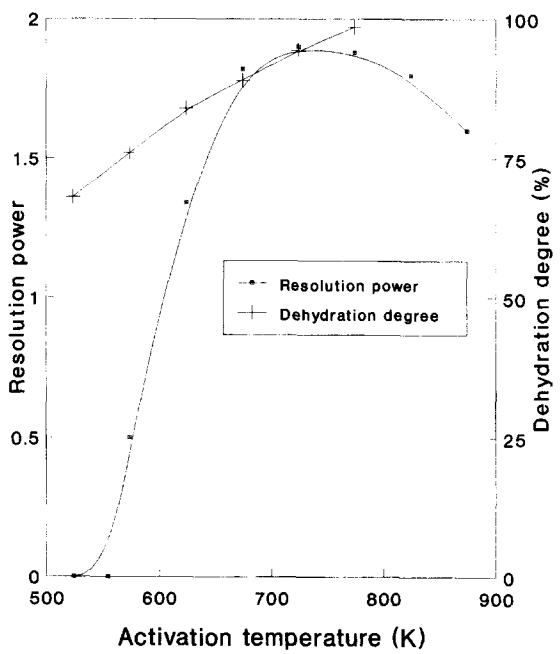

Fig. 4. Effect of the activation temperature on the dehydration and the resolution power of CLI.

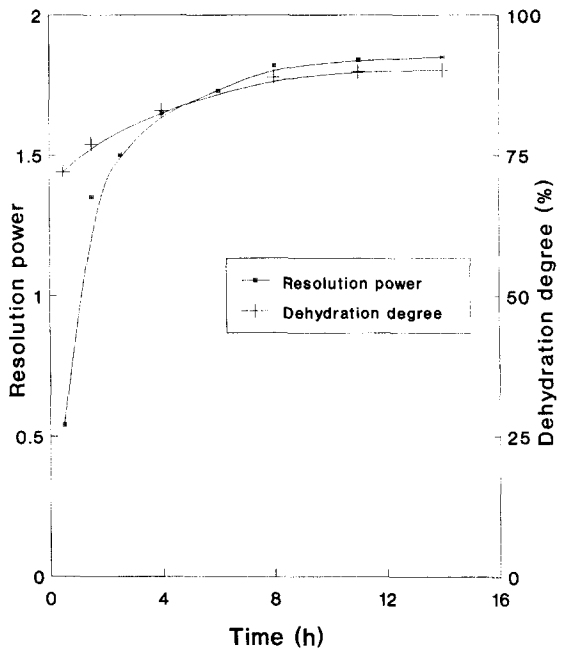

Fig. 5. Effect of the time of heating at 673 K on the dehydration and the resolution power of CLI.

when the zeolitic water is eliminated. In addition, as indicated in Fig. 5 for the sample activated at 673 K, the optimum separation capacity is reached after 8 h of treatment, when the water loss is about 90%.

Since the thermal stability of clinoptilolite depends on its chemical composition, in particular on the Ca_Z^{2+}/K_Z^+ ratio [14], the crystallinity of the samples activated at temperatures between 573 and 873 K for 8 h, was checked by XRD. The degree of crystallinity was estimated from the relative intensities of the most characteristic reflections of clinoptilolite ($2\theta = 9.92°$; 22.43° and 30.50°), taking as reference the intensities of these reflections of the sample heated at 393 K. The relative intensities were higher for the sample activated at 573 K (for example, for $2\theta = 9.92°$, $I/I_0 = 1.20$), as a consequence of the elimination of the water molecules from the channels of the framework. Above 773 K, a progressive decrease of the relative intensity of the diffraction lines occurs (63% and 32% at 823 K and 873 K, respectively), indicating that a partial breakdown of the structure takes place. This result would explain the lower values of

$R_{O/N}$ shown by such samples (see Fig. 4). Therefore, a treatment at 673 K during 8 h, under flow of nitrogen, was initially selected to activate the samples used in this work.

Since the breakdown temperature depends also on the nature of the major countercation [15], the crystallinity of the enriched cationic samples heated at 673 K was also tested. In these cases, the crystallinity was calculated from the sum of the intensities of the reflections at $2\theta = 9.92°$, 22.43° and 30.50°, taking as reference the sum of the intensities of the same reflections in the sample heated at 393 K. Previously, it was confirmed that the cation-exchange does not substantially modify the diffraction pattern of clinoptilolite. The data in Table 5 reveal that Ba-CLI, K-CLI, Cs-CLI and NH_4-CLI (actually, this form heated at 673 K becomes H-CLI) are very stable at 673 K, while the loss of crystallinity of samples Mg-CLI, Ca-CLI and Na-CLI is slightly higher. However, even for these last samples the content of zeolite phase is high enough to be practically responsible for their sieving properties.

4.3. Adsorptive capability

The adsorptive capability of the zeolite samples for CO, O_2, N_2, and CH_4 was characterized by the *specific retention volume*, which was calculated at different temperatures between 298 and 373 K, from the equation

$$V_g = t_r(F/w)(273/T_c) \quad (4)$$

where V_g (STP $cm^3 \cdot g^{-1}$) is the specific retention volume, t_r (min) the adjusted retention time with respect to helium, F (STP $cm^3 \cdot min^{-1}$) the carrier gas flow, w (g) the mass of zeolite in the column and T_c (K) the column temperature [21]. The absolute retention time (t') is the time elapsed between the emergence of the peak maximum of a solute A and the injection of the sample. So, $t_r = t_A' - t_{He}'$.

Table 5
Relative crystallinity of the enriched clinoptilolites heated at 673 K [a]

Sample	Crystallinity [a] (%)
H-CLI	92
Na-CLI	84
K-CLI	90
Cs-CLI	91
Ca-CLI	83
Mg-CLI	82
Ba-CLI	88

[a] Crystallinity of respective samples dried at 393 K = 100.

Among the impurities present in clinoptilolite, only mordenite could exhibit adsorptive properties and consequently modify the adsorptive capacity of clinoptilolite. However, mordenite is present in all the samples at a low level and therefore its influence, if any, would not significantly change the conclusions of this work.

To have access into the clinoptilolite channel, the critical size of the guest molecule must be lower than the critical dimension for entry of the zeolite, which is larger than the computed crystallographic pore size [23,24]. Table 6 summarizes the dimensions for CH_4, CO, N_2 and O_2, based on Pauling's values of bond lengths and Van der Waals radii of atoms and molecules [1]. The value given for CH_4 takes into account the tetrahedral structure of this molecule, while the values for CO, N_2 and O_2 correspond to the cross-sectional diameter, which is the critical dimension for penetrating the zeolite by dumbbell-shaped molecules.

When the zeolite channels are open enough to allow the free circulation of a guest molecule, V_g is related to the electrostatic interaction of the molecule with the adsorption centres of the zeolite. The strength of such interaction depends mainly on [25]: (a) the overall intensity of the local electrostatic field originating from the ionic nature of the zeolite framework, and (b) the polarity (dipole and quadrupole moments) and/or polarizability (induced dipole) of the guest molecule. In addition, depending on the structure and topology of the zeolite, the volume and location of the countercations may significantly modify the values of V_g. Thus, when the critical dimension of the molecule is close to the dimension for entry of the zeolite, the rate of adsorption is controlled by the resistance to diffusion.

When the access to the adsorption sites is not hindered, we can expect from the electric moments of CO, CH_4, N_2 and O_2 (Table 6) that the energy

Table 6
Physical characteristics of the adsorbates

Molecule	Dipole (debye)	Quadrupole ($Å^3$)	Polarizability ($Å^3$)	Kinetic diameter (Å)	Critical diameter (Å)
CO	0.12	0.33	1.60	3.76	4.2 × 3.7
CH_4	–	–	2.60	3.80	4.4
N_2	–	0.31	1.40	3.64	4.0 × 3.0
O_2	–	0.10	1.20	3.46	3.9 × 2.8

of the host–guest bond would decrease in the order $CO > CH_4 > N_2 > O_2$. In spite of the non-polar character of methane, this molecule interacts strongly with the zeolite due to its high polarizability, in such a way that its interaction energy is higher than the interaction energy for N_2 and O_2, produced by the polarizability plus the quadrupole moment of these molecules. With regard to the CO molecule, the relatively low difference between its polarization energy and that of CH_4, due to the lower polarizability of CO, is exceeded by the contribution of its quadrupole and permanent dipole moments. In general, this latter is the most important electrical component of the overall interaction energy [1,24,26].

As shown in Table 7, at 298 K, CO, N_2 and O_2 elute in the expected order, whereas methane does not. In particular, the V_g values of methane on Ca-CLI, Na-CLI, Mg-CLI and CLI, are even lower than those of O_2, while the values for H-CLI and Cs-CLI are slightly higher than those of CO. The V_g's of O_2 and N_2 on Ca and Na-CLI are also lower than those expected from the polarizing power of the cations (Table 4), and very similar to those obtained on Cs-CLI. Note that these anomalous values of V_g occur on samples in which the major countercation occupies the M(1) and M(2) sites.

Table 7
Specific retention volumes of CO, CH_4, N_2 and O_2 for the exchanged clinoptilolites at 298 K

Sample	V_g ($cm^3\ g^{-1}$)			
	CO	CH_4	N_2	O_2
H-CLI	26.6	28.1	8.6	5.0
Na-CLI	83.0	2.3	4.2	2.5
K-CLI	74.1	26.4	20.2	6.8
Cs-CLI	10.7	11.6	4.4	2.8
Nat-CLI	149.4	2.7	18.2	4.2
Mg-CLI	488.1	1.5	24.4	6.0
Ca-CLI	263.1	0.0	6.6	2.6
Ba-CLI	605.6	504.6	109.0	15.7

In most of the cases, CO exhibits the highest values of V_g (see Table 7), due to its permanent dipole moment. On the other hand, its V_g increase in the order: Cs-CLI < H-CLI < K-CLI < Na-CLI < Ca-CLI < Mg-CLI < Ba-CLI. Except for Ba-CLI, this sequence coincides with the increasing order in the ϕ values of the cations. There is a significant difference between the V_g's of O_2 and N_2 for K-CLI, Mg-CLI and, particularly, Ba-CLI, indicating that an efficient O_2/N_2 separation could be achieved on these samples. A similar behaviour for the K form of different clinoptilolites was also observed by other authors [6,19].

These findings are valid for the temperature range analyzed, as shown in Fig. 6, where $\ln V_g$ has been plotted as a function of $1/T$ for the different samples. The experimental data fit Eq. 5, which is valid at low coverage [19]

$$\ln V_g = (-\Delta H/RT_c) + C \quad (5)$$

In this equation, ΔH is the isosteric enthalpy of adsorption ($kJ \cdot mol^{-1}$), and R the gas constant. From the slope of the straight lines, the values of ΔH summarized in Table 8, which are characteristic for physisorption [1], were calculated. For each clinoptilolite sample, the values of ΔH decrease in the order $CO > N_2 > O_2$, similarly to the V_g values, as a consequence of the parallel decrease of the electric moments of the gas molecules. With regard to the major countercation in the zeolite, the adsorption enthalpy for CO increases in the order $Cs^+ < H^+ < K^+ < Na^+ < Ba^{2+} < Ca^{2+} < Mg^{2+}$ (Table 8). This order correlates satisfactorily with

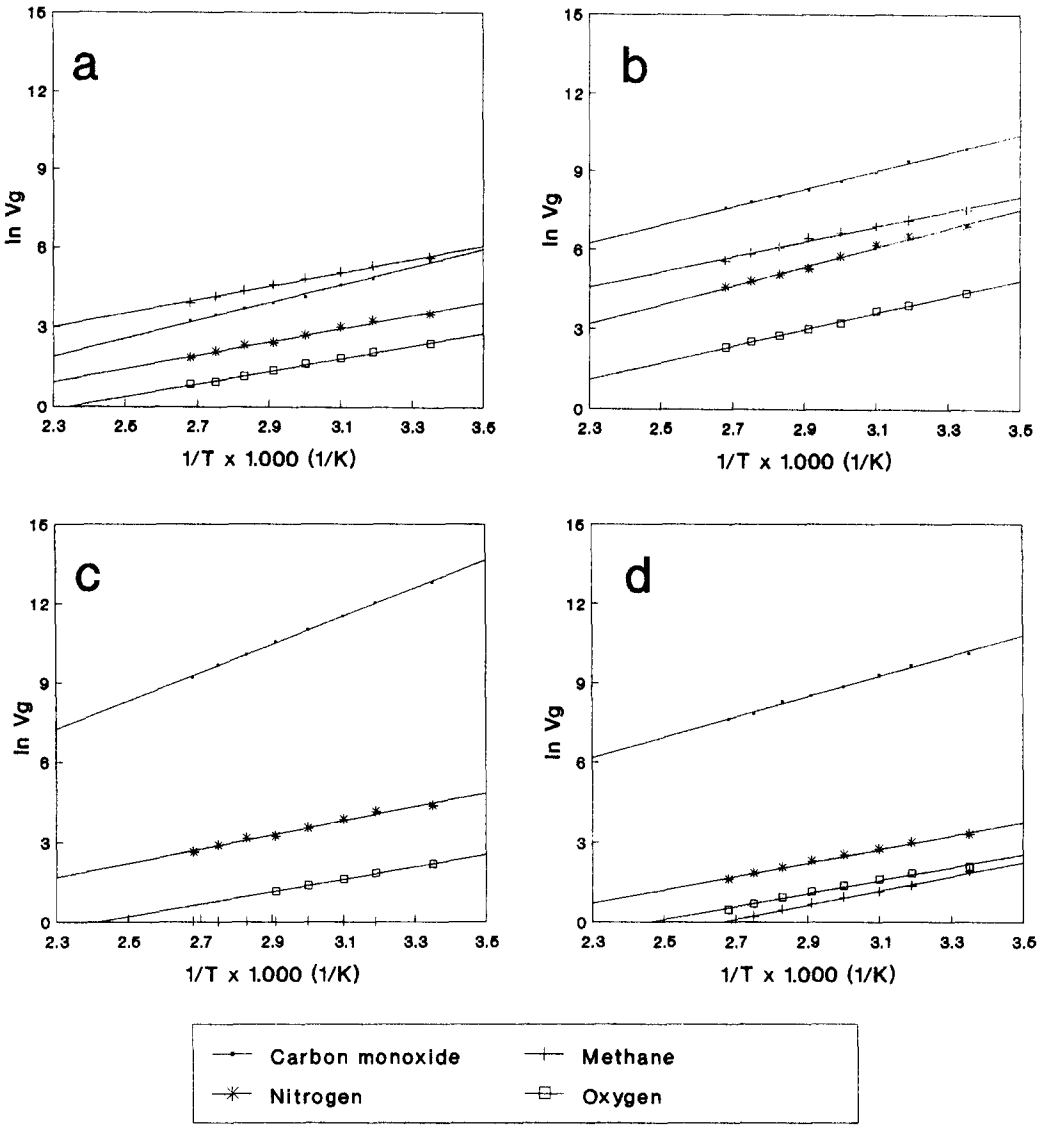

Fig. 6.

the strength of the induced local electrostatic field of the respective countercations (Table 4).

On the other hand, in spite of the high polarizability of methane, the low values of V_g and ΔH on Ca-CLI, Mg-CLI and Na-CLI indicate that the adsorption of this molecule on theses samples is governed by steric factors rather than by electrostatic interactions. In other words, the access of the guest molecule to the adsorption sites inside the channels is strongly hindered. In consequence, the above experimental results suggest that the effective pore size of Mg-, Na- and Ca-CLI are lower than 4.4 Å. This means that, in spite of the fact that Na^+, Ca^{2+} and Mg^{2+} have ionic radii smaller than those of K^+ or Cs^+, they are more effective blockers than these last cations. This is because K^+ and, consequently, Cs^+ preferentially occupy the M(3) sites in the channel C, preventing the neighbouring M(1) sites from further cation accommodation [14,17]. In these con-

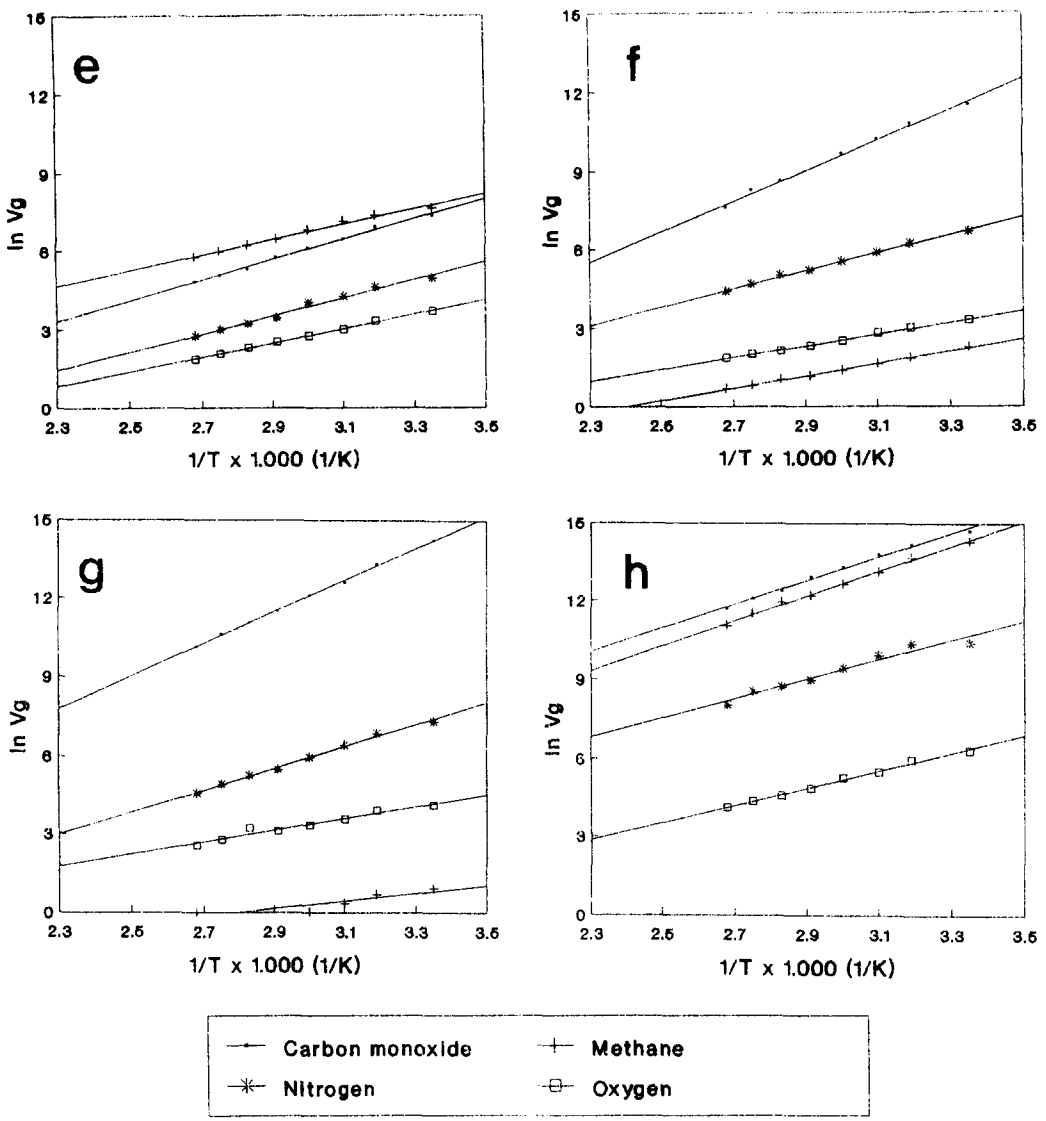

Fig. 6. Plots of Eq. 5 to calculate ΔH from the V_g's for the adsorption of CO, N_2, O_2 and CH_4 on: (a) Cs-CLI, (b) K-CLI, (c) Ca-CLI, (d) Na-CLI, (e) H-CLI, (f) CLI, (g) Mg-CLI and (h) Ba-CLI.

ditions, methane may easily diffuse through the channels A and B and have access to the adsorption sites of clinoptilolite. In Ca-CLI and Na-CLI, on the contrary, it is probable that a high population of Ca^{2+} and Na^{+} cations on M(1) and M(2) sites, respectively, restricts the diffusion of methane along the channels A and B and through the intersections of such channels with channel C [9,10]. With regard to Mg^{2+}, its preferential location at the M(4) sites strongly hinders the movement of methane along channel A.

It is interesting to point out that except for Ba-CLI, the ΔH values of CH_4 are very similar for all the samples and lower than those expected from the ϕ values of the cations (Table 4). These results, together with those of V_g, confirm that the adsorption of methane on these samples, particularly on Mg-CLI and Na-CLI, is controlled by the

Table 8
Adsorption enthalpies of CO, CH_4, N_2 and O_2 on the exchanged clinoptilolites

Sample	ΔH (kJ mol^{-1})			
	CO	CH_4	N_2	O_2
H-CLI	31.7	26.0	27.7	24.3
Na-CLI	37.2	20.9	21.6	17.8
K-CLI	33.2	22.9	29.2	24.5
Cs-CLI	26.8	22.0	23.9	21.6
Nat-CLI	50.3	21.8	31.9	30.6
Mg-CLI	51.8	22.9	35.7	30.1
Ca-CLI	46.0	–	21.7	21.7
Ba-CLI	43.1	40.7	35.9	27.3

diffusion rate rather than by electrostatic interactions. The sample Ca-CLI, for which V_g is zero in the temperature range analyzed, is a limiting case of this behaviour. A similar explanation can be given for the adsorption of N_2 and O_2 on Ca- and Na-CLI. The V_g as well as the ΔH values are very similar to those obtained for Cs-CLI, in spite of the significant differences between the polarizing power of the countercations. The value of V_g of methane on H-CLI, higher than on CLI, can be related to the partial decationation and subsequent substitution of Na_Z^+ and Ca_Z^{2+} by protons, which enables the access of methane to the channels.

The highest V_g and ΔH values for the four gases on Ba-CLI arise from a strong electrostatic field–guest molecule interaction and the absence of diffusional limitations. Since the ionic radius of Ba^{2+} (1.35 Å) is very similar to that of K^+, the high V_g value for methane on Ba-CLI can only be explained if one accepts that Ba^{2+} is located in M(3) sites. It must be pointed out that the retention volume of all the gases on sample CLI falls between those of the monovalent and bivalent cations, probably due to the presence of several cations with different valence and in different concentration, which results in an average in-between formal valence.

5. Conclusions

Clinoptilolite from Castilla (Cuba), activated at 673 K, is an adequate molecular sieve to separate N_2 and O_2 from air, and less expensive than the synthetic zeolites. Ion exchange treatments with NH_4^+, Na^+, K^+, Cs^+, Mg^{2+}, Ca^{2+} and, particularly Ba^{2+}, substantially modify its adsorptive capability and enables a suitable separation of gases such as N_2, O_2, CO and CH_4. The nature, polarizing power and location of the cations in the framework play an important role on the adsorption capacity of clinoptilolite towards O_2, N_2, CO and CH_4.

Acknowledgment

The authors gratefully acknowledge financial support from Comision Mixta Hispano-Cubana. Prof. J.A. González thanks the Spanish Ministerio de Educación y Ciencia for support to a year's sabbatical leave.

References

[1] D.W. Breck, Zeolites Molecular Sieves, Wiley-Interscience, New York, 1974.
[2] R.M. Barrer and B. Coughlan, Molecular Sieves, The Society of Chemical Industry, London, 1968, p. 141.
[3] D. Kalló, J. Papp and J. Valyon, Zeolites, 2 (1982) 13.
[4] J.A. González, G. Llabre, N. Travieso, M. Barrameda and J.C. Romero, in G. Rodriguez and J.A. González (Editors), Proc. 3rd. Int. Conf. Natural Zeolites, Havana, Vol. I, 1991, p. 142.
[5] H. Minato and T. Tamura, in L.B. Sand and F.A. Mumpton (Editors), Natural Zeolites. Occurrence, Properties, Uses, Pergamon Press, Oxford, 1978, p. 509.
[6] T.M. Galabova and G.A. Haralampiev, in R.P. Townsend (Editor), Properties and Aplications of Zeolites, The Chemical Society, London, 1979, p. 121.
[7] H. Minato, in G. Rodriguez and J.A. Gonzalez (Editors), Proc. 3rd. Int. Conf. Natural Zeolites, Havana, Vol. I, 1991, p. 3.
[8] G.V. Tsitsishvili and T.G. Andronikashvili, J. Chromatogr., 58 (1971) 39.
[9] M.W. Ackley and R.I. Yang, AIChE J., 37 (1991) 1645.
[10] M.W. Ackley and R.T. Yang, Ind. Eng. Chem. Res., 30 (1991) 2523.
[11] M.W. Ackley, R.F. Giese and R.T. Yang, Zeolites, 12 (1992) 780.
[12] A. Arcoya, J.A. Gonzalez, N. Travieso and X.L. Seoane, Clay Miner., 29 (1994) 123.
[13] A. Alberti, Tschermaks Mineral. Petrogr. Mitt., 22 (1975) 25.
[14] K. Koyama and Y. Takeuchi, Z. Kristallogr., 145 (1977) 216.

[15] G. Gottardi and E. Galli, Natural Zeolites, Springer-Verlag, Berlin, 1985, p. 28.
[16] T. Ambruster, Am. Mineral., 78 (1993) 260.
[17] K. Sugiyama and Y Takeuchi, Stud. Surf. Sci. Catal., 28 (1986) 449.
[18] J.R. Smyth, A.T. Spaid and D.L. Bish, Am. Mineral., 75 (1990) 522.
[19] G.V. Tsitsishvili, T.G. Andronikashvili, Sh.D. Sabelashvili and N.A. Osipova, J. Chromatogr., 130 (1977) 13.
[20] G.V. Tsitsishvili, in L.B. Sand and F.A. Mumpton (Editors), Natural Zeolites. Occurrence, Properties, Uses, Pergamon Press, Oxford, 1978, p. 397.
[21] J. Tranchant, in J. Tranchant (Editor), Manuel Pratique de Chromatographie en Phase Gaseuze, Masson, Paris, 1968, p. 23.
[22] R.L. Ward and H.L. McKague, J. Phys. Chem., 98 (1994) 1232.
[23] J.G. Bendoraitis, A.W. Chester, F.G. Dwyer and W.E. Garwood, Stud. Surf. Sci. Catal., 28 (1986) 669.
[24] R.M. Barrer, in F. Râmoa-Ribeiro, A.E. Rodrigues, L. Deane Rollmann and C. Naccache (Editors), Zeolites: Science and Technology, Martinus Nijhoff, The Hague, 1984, p. 227.
[25] J.V. Smith, in J.A. Rabo (Editor), Zeolite, Chemistry and Catalysis, American Chemical Society, Washington, DC, 1976, p. 69.
[26] M.R. Barrer, J. Colloid Interface Sci., 21 (1966) 415.